AN ABSTRACT OF THE THESIS OF

ALAN B CHAMBERS (Name) for the Ph. D. (Degree)

in Mechanical Engineering (Major) presented on Aug. 9, 1967

Title: A MODEL OF CILIARY STREAMING IN THE RESPIRATORY SYSTEM

Abstract approved: Redacted for privacy

Richard W. Boubel

The respiratory tract is lined with a mucous blanket which is motivated by a ciliated epithelium. This blanket includes a lower serous layer of fluid through which the cilia beat and an upper viscid layer into which particulates from the inhaled air are deposited. The movement of the mucous blanket comprises the ciliary stream and is the primary mechanism responsible for clearance of particulates from the respiratory system.

A mathematical model was developed representing a small segment of the ciliary stream and describing the movement of the upper viscid layer of mucus and the tips of the cilia which project through the serous fluid into the upper viscid layer. The cilia tips are represented as a continuous surface which oscillates along the lower edge of the viscid mucous layer. The mucus was assumed to behave as a Bingham plastic.

An analytical solution is presented for the steady-state

component of the mucous velocity and both numerical and analytical solutions are presented for the time-dependent component, which is a parabolic differential equation with a moving boundary.

Conclusions indicated that in order to obtain a mucous flow in the positive direction, the tips of the cilia cannot be in constant contact with the upper fluid layer. The serous layer, which has been almost completely neglected in previous research, appears to be at least as important to the system as the upper viscid layer. Furthermore, the thickness of the serous layer may be the most important single parameter of the system.

A Model of Ciliary Streaming in the Respiratory System

by

Alan B Chambers

A THESIS

submitted to

Oregon State University

in partial fulfillment of
the requirements for the
degree of

Doctor of Philosophy

June 1968

APPROVED:

Redacted for privacy

Professor of Mechanical Engineering
in charge of major

Redacted for privacy

Head of Department of Mechanical Engineering

Redacted for privacy

Dean of Graduate School

Date thesis is presented Aug. 9, 1967

Typed by Marion F. Palmateer for Alan B Chambers

ACKNOWLEDGEMENTS

The author gratefully acknowledges Dr. Richard Boubel for his consistent support throughout this research project and the Public Health Service for financial assistance under fellowship 5 F3 AP 29, 825-02.

TABLE OF CONTENTS

LIST OF FIGURES

LIST OF TABLES

A MODEL OF CILIARY STREAMING IN THE RESPIRATORY SYSTEM

I. INTRODUCTION

> . . . if present trends continue (lung cancer) will claim the lives of more than 1, 000, 000 present school children in this country before they reach the age of 70 years. . . . (American Public Health Association, 1959, p. 1698)

The increasing rate of deaths due to pulmonary diseases (with the exception of tuberculosis) has attracted widespread attention in recent years: in the State of Oregon 6. 6% of all deaths reported in 1956 were attributed to pulmonary diseases (Oregon State Board of Health, 1958), however, by 1965 this figure had increased to 7. 9% (Oregon State Board of Health, 1966); similarly, on the national level the percentage of deaths attributed to pulmonary diseases increased from 5. 62% in 1950 (U. S. Dept. H. E. W., 1953) to 8. 0% in 1964 (U. S. Dept. H. E. W., 1966). Lung cancer, chronic bronchitis, and emphysema account for a large portion of these increasing figures. In fact, lung cancer alone was responsible for 50, 598 deaths in the United States in 1964, a toll higher than that exacted by all motor vehicle accidents (U. S. Dept. H. E. W., 1966) and more than 100 times that exacted by all our earthquakes, floods, and tornados added together (U. S. Weather Bureau, 1964).

Purpose of This Study

Impairment of the primary defense mechanism of the lung--the ciliary streaming action--is generally considered to be the leading cause of the increases in pulmonary disease (Blake, 1964; Miller and Goldfarb, 1965; Ballenger and Orr, 1963; Hatch and Gross, 1964; Bang, 1961). The respiratory system functions as an extremely efficient filter for the removal of particulates from the inhaled air; consequently, even a small decrease in the efficiency of the ciliary streaming action may cause a harmful accumulation of foreign and potentially toxic materials.

The purpose of this thesis is to consider, using a mathematical model, some of the interrelationships of the parameters of the ciliary stream and thus to gain a better understanding of the manner in which this system operates.

Pulmonary Deposition and Clearance

The average adult breathes 10 to 20 cubic meters of air a day. "Ordinarily, this volume of air contains approximately 1,000 billion particles with a total weight between one and two milligrams" (Mitchell and Tomashefski, 1964, p. 5). It is possible, however, that in a "moderately dirty community atmosphere" an individual will inhale ten milligrams of particulate matter per day (Hatch and

Gross, 1964, p. 69). In extremely dusty areas, such as poorly ventilated mines and industries, the particulate concentration often approaches 10^7 particles per cubic centimeter and the mass concentration may exceed 100 milligrams per cubic meter (Morrow, 1967), so a person might inhale over a gram of particles a day.

A large portion of these inhaled particulates are deposited in the respiratory tracts. The amount and site of particulate deposition is dependent primarily on the size and density of the particles and on the rate and depth of respiration. In the upper respiratory tract (that area above the pharynx, Figure 1) removal efficiency is essentially 100% for particles eight microns and larger; however it drops rapidly with reduction of particle size and is nearly zero at one or two microns (Figure 2). With essentially 100% removal of particles eight microns or larger in the upper respiratory tract, the probability of penetration of these coarse particles to the pulmonary air spaces is negligible. As indicated on Figure 2, the particles most likely to be deposited in the pulmonary air spaces are those within the size range one to two microns and those below 0.2 microns. When breathing through the open mouth or when smoking, however, essentially all the particulates (including those eight microns and larger) are introduced directly into and deposited in the lower respiratory tract.

Total deposition in the respiratory tract increases as breathing

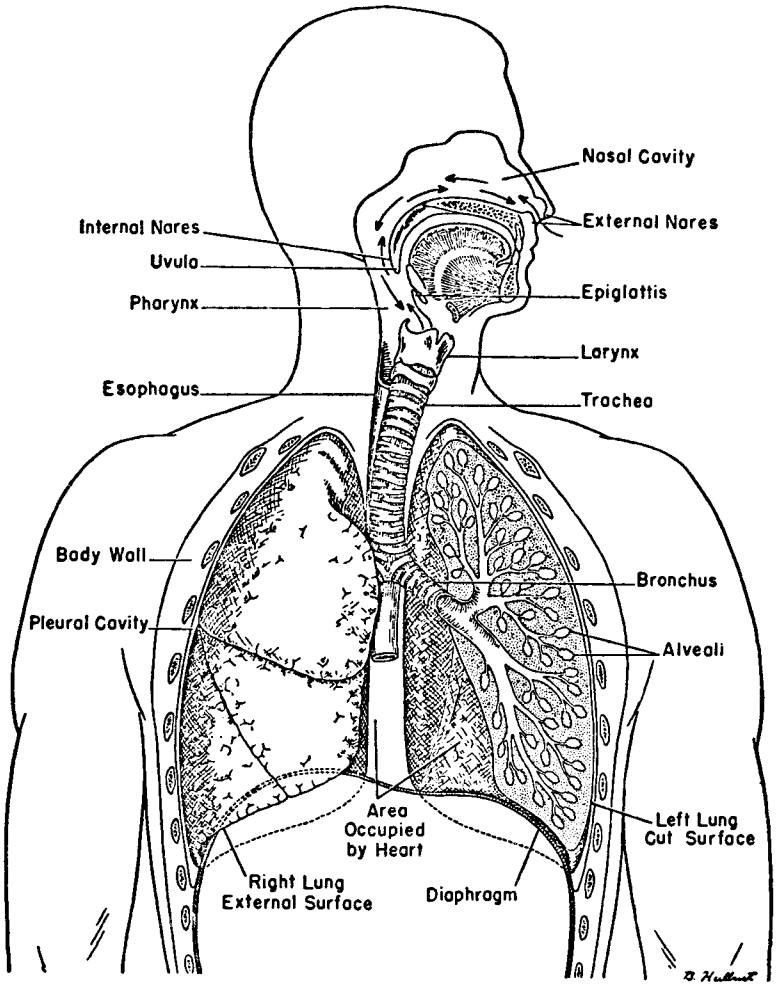

Figure 1. The respiratory system. (Villee, 1960, p. 267)

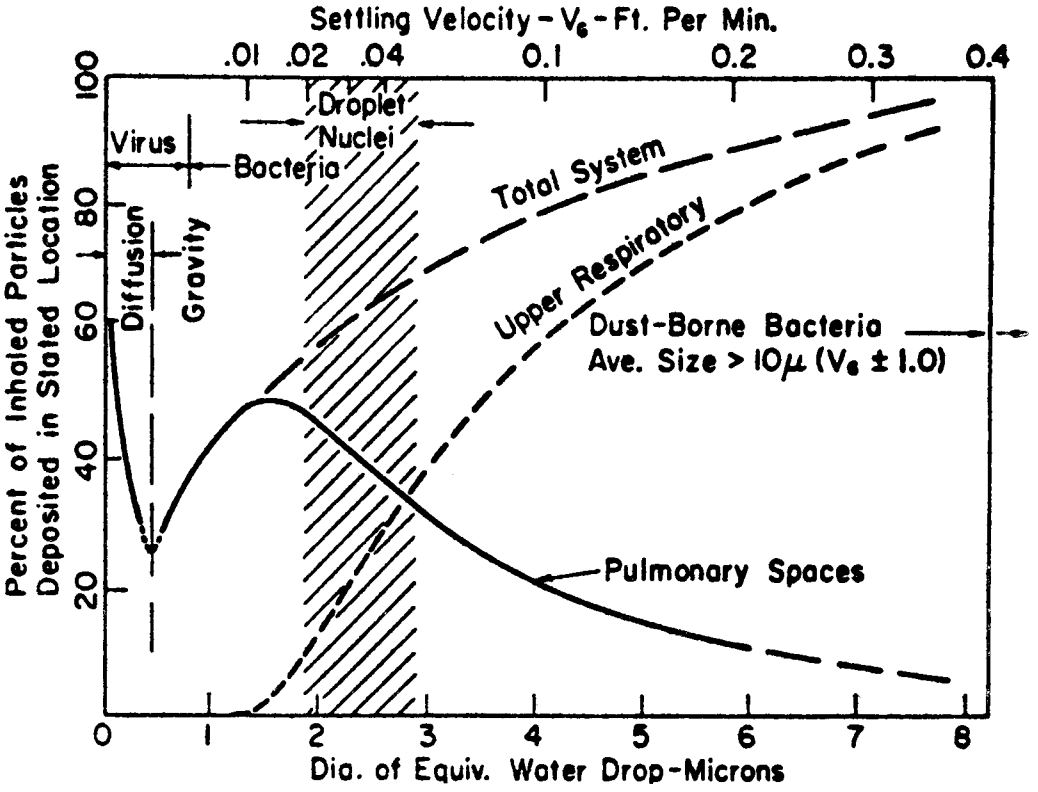

Figure 2. Total and regional deposition of inhaled particles in relation to the aerodynamic particle size. (Hatch, 1961, p. 238)

frequency decreases. This occurs primarily for two reasons: the transit time for the air (and particles) into and out of the system is increased, thus providing a longer time for the aerosols to settle out; and tidal volume increases as respiratory frequency decreases such that a larger portion of the inspired air reaches the distal portion of the lung (Hatch, 1961).

The lung rids itself of particulates primarily in two ways. Those which have been deposited in the respiratory tract above the alveoli are carried by a moving layer of mucus from the site of initial deposition to the esophagus where they are passed into the gastro-intestinal tract or expectorated. Those which have been deposited in the alveoli are, at least in part, picked up by phagocytes. Some of the latter are transported to the lymphatics and some to the terminal bronchioles where they are carried in the mucous flow. These two mechanisms are assisted to some degree by respiratory excursions, peristaltic waves, and cough (Ballenger, 1960); however, the extent to which these assisting actions play a role in particulate clearance has not been determined.

The thin layer of mucus covering the respiratory passages has a "stickiness" or adhesive quality which traps foreign particles as they impinge on its surface. This quality, as well as the rheology of the mucus (which will be discussed), is due, at least in part, to its protein and carbohydrate polymer structure.

This mucous layer derives its movement from the ciliated epithelium. Its progress is ceaseless and always toward the pharynx: that is, in the upper respiratory tract the action of the cilia moves the mucus posteriorly to the pharynx, and in the lower respiratory tract the movement is anterior to the upper end of the esophagus. Both the nasal mucus and that from the lower respiratory tract are normally swallowed when they reach the hypopharynx (Proctor, 1964).

Approximately 90% of the inhaled particulates are cleared by the moving mucous blanket; the remaining 10% are cleared to the lymphatics by other transport mechanisms (Gross, 1964).

Cilia and the Ciliary Stream

A ciliated epithelium (Figure 3) lines the entire respiratory tract, the eustachian tubes, and the paranasal sinuses except the alveoli, the vocal cords, the epiglottis, the oropharynx, the olfactory area, the crypts of the lymphoid masses, and between the anterior ends of the nasal turbinates and the nostrils (Proctor, 1964). The cilia are very densely positioned on the epithelium, ranging from approximately 10 to 35 per square micron (Engström and Wersäll, 1952; Rhodin and Dalhamn, 1956; Lucas, 1932). Their diameters range from 0.15 to 0.3 microns (Rhodin and Dalhamn, 1956), and lengths range from six to nine microns (Lucas, 1932; Proctor, 1964).

The cilia are rigid as they move rapidly forward in an

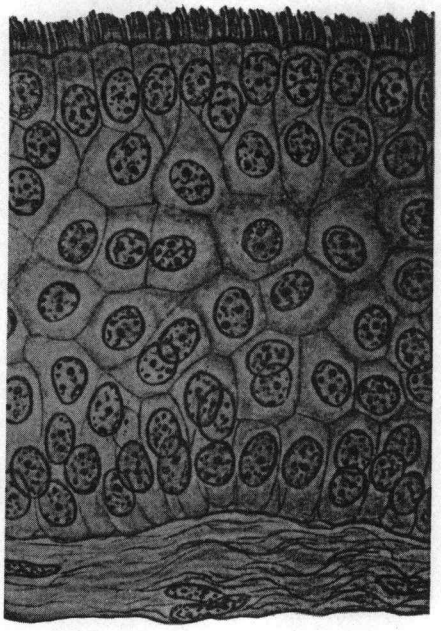

Figure 3. Stratified columnar ciliated epithelium from the laryngeal surface of the epiglottis of a 31-week human embryo (795X). (Bloom and Fawcett, 1964, p. 62)

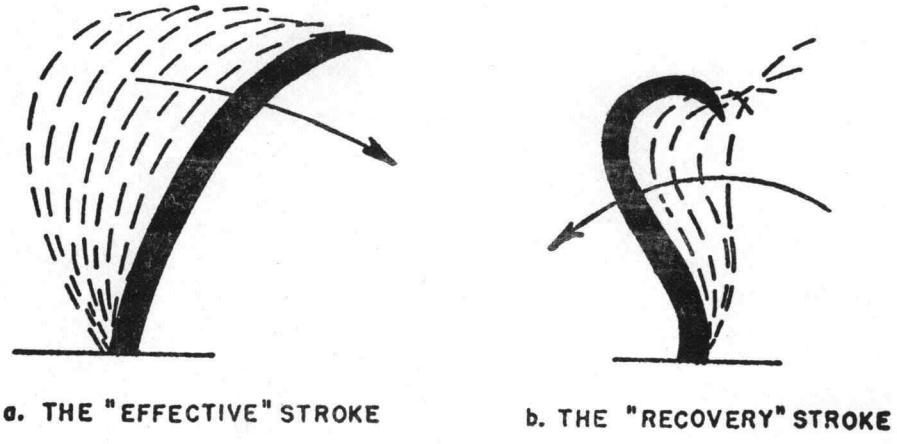

Figure 4. Effective and recovery stroke of human nasal cilium. (Proetz, 1953, p. 193)

"effective stroke" and are bent in a curved position during the slower "recovery stroke" (Figure 4). These strokes are in the same plane and perpendicular to the long axis of the cilium. The stroke frequency is inversely proportional to the size of the cilium and is very sensitive to changes in temperature and moisture (Ballenger, 1949). It may be as high as 1500 beats per minute with a forward to reverse phase ratio of 1:2 to 1:5 (Dalhamn and Rhodin, 1956). It is this whipping action of the cilia that causes the mucus to flow.

The thin layer of mucus overlying the respiratory epithelium, motivated by ciliary action, constitutes the ciliary stream. The stream flows constantly, regardless of body position, always toward the pharynx. The nonciliated areas enumerated previously, and other small nonciliated islands, may still be covered by the flowing mucous blanket because of traction from adjacent ciliated areas (Proctor, 1964).

The mucous layer originates from three sources in the respiratory tract:

> (1) The mucinous secretions of goblet cells in the mucosa as well as from the submucosal mucous glands of the tracheo-bronchial tree,
> (2) The secretions of certain apocrine cells in the respiratory bronchioles and
> (3) The alveolar film of fluid.
> (Gross, 1964, p. 996)

The total volume output of this fluid is normally 0. 1 to 0. 3 milliliters per day per kilogram of body weight (Toremalm, 1960), which is

about 7 to 20 milliliters per day for an average human adult.

The mucous blanket is composed of two parts (Figure 5): "an overlying viscid sheet and a layer of serous fluid which furnishes the medium in which the cilia vibrate" (Lucas and Douglas, 1934, p. 531). It is thought that the viscid upper layer may be the fluid derived from the mucous glands and that the thin less viscous portion may be the fluid originating in the alveoli (Gross, 1964).

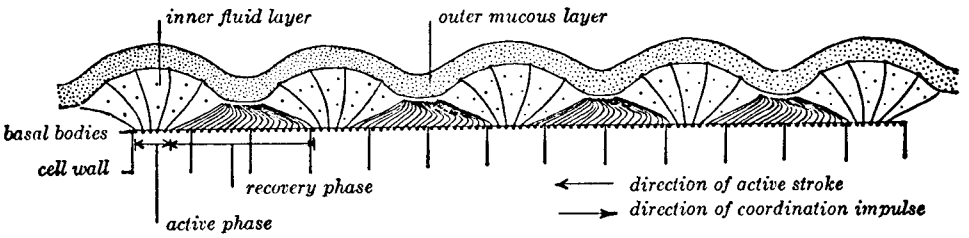

Figure 5. Diagram of ciliary action showing the location of the inner and outer fluid layers in relation to the vibrating cilia. (Lucas and Douglas, 1934, p. 532)

It is the upper viscid layer of mucus into which particulates are normally deposited and remain until swallowed or expectorated. This layer is normally about five microns thick, although under certain pathological conditions, may be as thick as 25 microns (Dalhamn, 1956) (Figures 6 and 7). However, even under normal conditions the thickness may vary as the layer moves through the tracheo-bronchial tree due to the progressive narrowing of the mucous flow

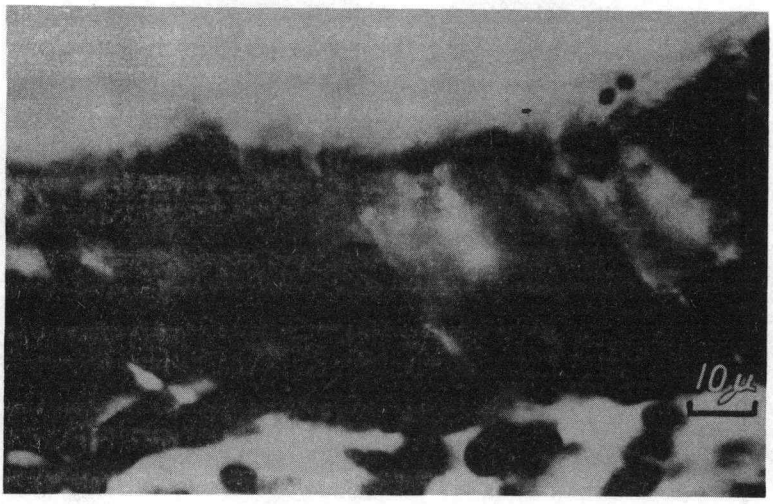

Figure 6. Freeze-fixed mucosa from a healthy rat. The mucous blanket is distinguishable above the cilia (800X). (Dalhamn, 1956, p. 90)

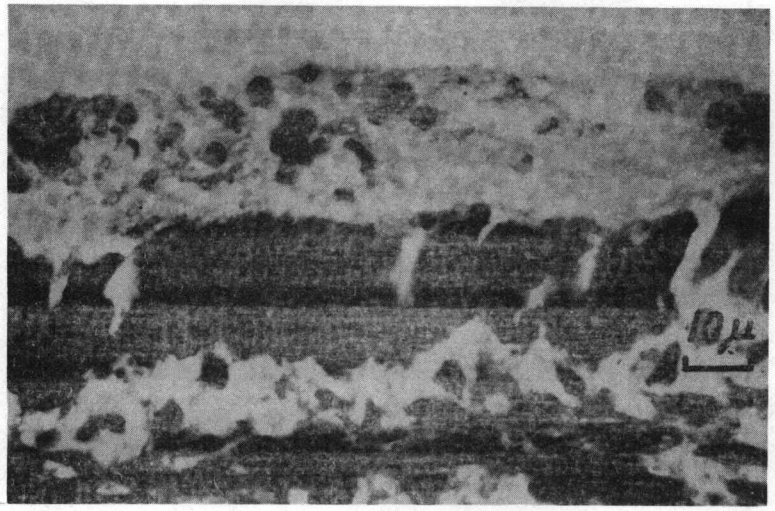

Figure 7. Freeze-fixed mucosa from a rat exposed for 67 days to 11.5 ppm SO_2. The mucous layer contains numerous cellular elements (800X). (Dalhamn, 1956, p. 90)

streambed (Hilding, 1957).

Various measurements of the speed of mucous flow have been made: they range from one millimeter or less per minute in the bronchioles and 10 to 15 millimeters per minute in the trachea (Hilding, 1963). Measurements have been made by placing particles of charcoal, graphite ink, or pollen dust on the mucous blanket or by using shed cells in the mucus as indicators of the flow (Dalhamn, 1956).

It should be noted, however, that the techniques themselves may be irritating to the system, thus affecting the measurements of flow. For example, when utilizing large particulates as indicators of flow, the velocity may be affected by the size of those particulates and the depth to which they penetrate the mucous layer. Furthermore, the rate of mucous flow cannot be used as a reliable indicator of ciliary activity for, although "mucous flow is never apparent where ciliary beat is absent, mucostasis may occur without any observable changes in ciliary beat frequency" (Carson, Goldhamer, and Weinberg, 1966, p. 937).

Retarded Flow and Mucostasis

Stasis of mucous flow will result if the cilia fail to perform normally and effectively, although it can also occur without a reduction in ciliary performance. Impairment of mucous flow has been

shown to occur because of experimental exposure to various irritating gases such as SO_2, ammonia, formaldehyde (Dalhamn, 1956), cigarette smoke (Dalhamn and Rylander, 1966) (Figure 8), and others (Batigelli, 1966).

> Slowing of the mucous stream starts a vicious cycle. As the stream moves more slowly it is exposed to inspired air currents for a longer time, gives up more of its water content, becomes more viscid, and is thus slowed still more. (Proctor, 1964, p. 328)

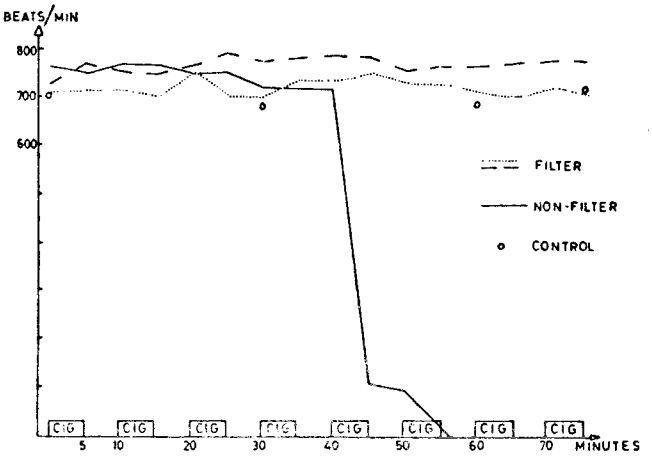

Figure 8. The effects of cigarette smoke on ciliary action. (Dalhamn and Rylander, 1964, p. 402)

Mucostasis or a retardation of mucous flow may permit an accumulation of inhaled debris in the respiratory tract. If this accumulation is bacterial, infection may result; moreover, if the debris is carcinogenic, cancer may result. Various pharmacological agents have been applied both directly and indirectly to the respiratory tract in order to alter mucous flow (Proctor, 1964): the effects may

be to alter cilia frequency, the ratio of forward to reverse phase, the rate of mucous secretion, viscosity, density, or numerous other parameters or combinations thereof. There is no knowledge, however, of which parameter or group of parameters should be altered (or to what magnitude) in order to optimize the clearance of mucus under various pathological conditions.

It is the purpose of this thesis, then, to consider some of the interrelationships of the parameters of the ciliary stream and thus to gain a better understanding of the manner in which this system operates.

II. THE MODEL

The model developed for use in this thesis represents a small segment of the ciliary stream and describes the movement of the upper viscid layer of mucus and the tips of the cilia which project through the serous fluid into this upper layer (Figure 9).

Basic Assumptions

Since the cilia are very densely packed on the epithelium (generally the distance between cilia is less than the diameter of one cilium), the cilia tips are represented in the model as a continuous surface which oscillates along the lower edge of the viscid mucous layer.

The oscillation of all the cilia in the respiratory tract is not synchronous; rather, the cilia beat in succession in one direction across the epithelium to give the appearance of metachronal waves. Each cilium is at a slightly different phase from its neighbors that lie in the line of wave transmission.

> The direction of the metachronal waves varies in different animals, but the direction of wave progression is usually constant for a given tissue. It may be in the direction of the effective stroke, or of the recovery stroke, or even laterally. (Rivera, 1962, p. 34)

It appears, then, that the metachronous nature of the movement of the cilia is not fundamental to the constant movement of the mucous

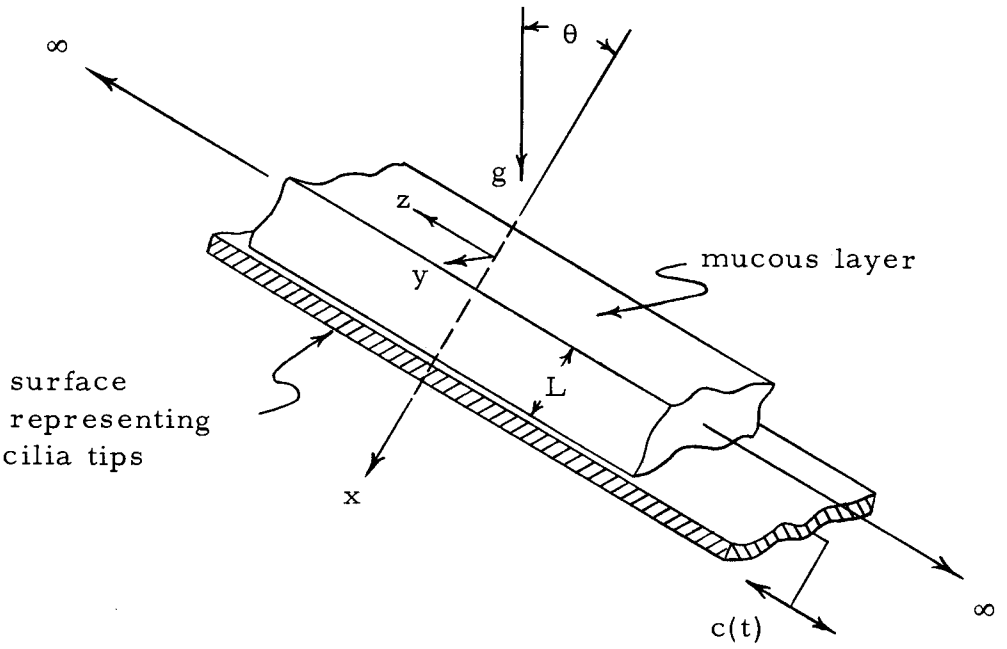

Figure 9. The model configuration.

Where,

θ = the angle of inclination of the x-axis (inward normal to the mucus) to the gravity vector, g

L = thickness of the mucous layer

c(t) = the oscillation of the inner surface depicting the movement of the cilia tips.

blanket. Therefore, for the purposes of this investigation, the oscillation of the surface representing the cilia is assumed to be independent of the coordinate position and, thus, time dependent only. Furthermore, the mucus is assumed to flow only in the direction of the cilia oscillation.

As noted previously, variations in the thickness of the mucous layer may occur during passage through the tracheo-bronchial tree due to progressive narrowing of the streambed. Even a slight change in thickness, however, would require passage through several centimeters of the tract, a distance which is several orders of magnitude greater than the thickness of the mucous layer. Thus, the length of the tract may be considered infinite, and any change in thickness may be considered negligible. Similarly, the radius of even the smallest of the ciliated passageways, the terminal bronchioles (radius of approximately 0.03 centimeters, Landahl, 1950), is several orders of magnitude greater than the thickness of the mucous blanket, so the curvature of the passageways also may be considered negligible.

In summary, then, the basic assumptions of the model are as follows:

1. The tips of the cilia represent a continous surface;
2. That surface oscillates as a function of time only;
3. Velocity occurs in the z-direction only;

4. The system extends to ± infinity in the z-direction;

5. The mucous layer is a constant thickness, L;

6. The curvature in the y-direction is negligible.

General Equations

Momentum equations for the mucous layer may be developed by applying Newton's Second Law to a differential fluid element. By equating surface and body forces to the change in linear momentum (inertial force) of the fluid element, the equations take the form

$$\rho \frac{Dv_i}{Dt} = - \rho \frac{\partial \Omega}{\partial x_i} + \frac{\partial \sigma_{ij}}{\partial x_j} \qquad \text{(Lamb, 1945, p. 576)}$$

where:

v_i = the velocity vector of a fluid element whose cartesian coordinates are x_i ;

Ω = the potential of a force field (i. e., gravity);

σ_{ij} = a stress tensor component;

ρ = the density of the fluid.

In order to solve this set of equations for a unique set of solutions corresponding to given boundary conditions, it is necessary to relate the stress field to the velocity field by an equation describing the mucous rheology.

Mucous Rheology

"Mucus is a complex polymeric material which is non-Newtonian in nature" (Barnett and Miller, 1966, p. 891). It is composed of approximately 2% solids, 3% mucin, and 95% water (Proetz, 1934). Mucin consists of a mucoprotein bound to a mucopolysaccharide in the form of a large polymer. These "mucus macromolecules are flexible, random-coiling... (and) form highly swollen, water-sequestering coils that vary in size substantially according to their precise ionic environment" (Merrill and Wells, 1961, p. 671).

The molecules may become entangled with one another forming a three-dimensional network in which disentangled molecules are contained. It is to be expected that the physical properties of the mucus are greatly affected by the relative quantities of entangled and disentangled molecules. The relative proportions can be determined by an equilibrium constant and may be expected to change under high stresses (Hahn, Ree, and Eyring, 1959).

Numerous measurements have been made of the physical properties of mucus, particularly of the viscosity. Few have considered, however, its polymeric structure or its non-Newtonian nature. Often, in fact, the mucous sample has been homogenized prior to analysis; this, of course, destroys whatever network formation may exist and precludes any valid observation of viscosity.

> A varying degree of recovery of the initial high viscosity occurs when the homogenized specimens are allowed to stand, and this appears to reflect partial restitution of the gel-structure. However, the primary structure of the intact mucus is largely lost. (White and Elmes, 1960, p. 259)

Furthermore, and with rare exception, the viscosity has been measured by an Ostwald viscometer or some other capillary device applicable only to Newtonian fluids (Merrill, 1955).

Wells, Denton, and Merrill (1961) seem to have been the first to consider the structure and composition of mucus in the design of their experiment to measure mucous viscosity. Using a cone plate viscometer, which is especially suitable for non-Newtonian fluids (McKennell, 1954), their analysis indicated that mucus is pseudoplastic in character.

More recently, Denton (1963) and Miller and Goldfarb (1965) indicated that mucus may have a "discreet yield point" below which flow will not occur. Miller and Goldfarb studied the stress vs. shear rate of strain for mucus: Figure 10 was presented as a typical set of rheology flow curves taken from mammalian mucus. Flow curve I corresponds to the initial shearing of the mucus, while curve II corresponds to a repeated shearing. This figure shows the stress necessary for flow and indicates that the bronchial mucus is thixotropic.

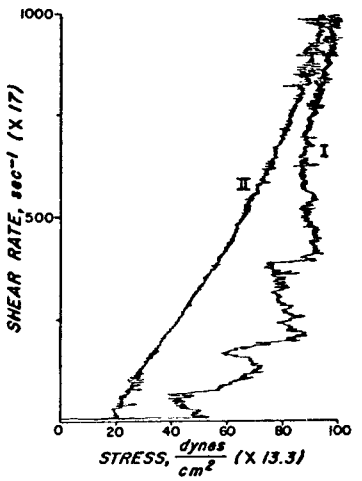

Figure 10. Rheological flow curve for a mucous sample. (Miller and Goldfarb, 1965, p. 136)

Under normal conditions the motion of the cilia is continuous and essentially non-stopping; consequently, the dependence of the mucous viscosity on repeated shearing (the thixotropic nature) may be such that the mucus obtains some steady state values for the relation of stress to rate of deformation. Noting the thixotropic nature of the mucus, Miller and Goldfarb (1965) postulated that the cilia, by their repeated application of stress, may "cause the mucus to be at the proper viscosity for optimum transport in the lumen" (p. 137). Thus, it seems reasonable to assume that the in vivo rheology of the mucus would correspond more closely to curve II than to curve I. Therefore, for the model used, curve II was considered to be descriptive of the rheology of the mucus.

The mucus is thus to be considered to exhibit the rheological properties of a Bingham material: the material at any point has zero

deformation rate until a certain combination of stresses at that point exceeds a critical value. Once the critical stress has been exceeded, flow begins and a linear relationship exists between the stress and the rate of deformation.

This rheological behavior was first described by Bingham in 1916. Later, Oldroyd (1947a) presented the rheology equations as follows:

$$2\mu d_{ij} = \left(\frac{\sqrt{J_2} - \Phi}{\sqrt{J_2}}\right) S'_{ij} \qquad \text{if} \quad \sqrt{J_2} \geq \Phi$$

$$d_{ij} = 0 \qquad \text{if} \quad \sqrt{J_2} \leq \Phi$$

where S'_{ij} is the deviatoric stress component derived from the stress tensor as follows:

$$S'_{ij} = \sigma_{ij} - \frac{1}{3}\delta_{ij}\sigma_{kk}$$

where δ_{ij} is the Kronecker delta and where d_{ij} is a component of the incompressible deformation rate tensor:

$$d_{ij} = \frac{1}{2}\left(\frac{\partial v_i}{\partial x_j} + \frac{\partial v_j}{\partial x_i}\right)$$

J_2 is the second (quadratic) invariant of the deviatoric stress tensor:

$$J_2 = \frac{1}{2} S'_{ij} S'_{ji}$$

and μ is the "plastic viscosity" of the material.

These equations show that no deformation occurs unless the combined stress, J_2, exceeds the critical value Φ. Alterations in the chemical or physical properties of the mucus may be reflected in changes of either or both μ and Φ. (Note also, that if Φ is zero the fluid is Newtonian.)

Thus, for the mucus under consideration any of the following conditions may exist:

μ low and Φ low = thin and flows readily

μ low and Φ high = will not flow readily, but will offer little resistance once flow is initiated

μ high and Φ low = thick and flows readily

μ high and Φ high = thick and does not flow readily

Equations of Motion

From the assumptions,

$$u_x = u_y = 0$$

$$\frac{\partial u_z}{\partial z} = 0$$

and

$$\sigma_{yx} = 0$$

$$\sigma_{yz} = 0$$

Excluding consideration of fields other than the gravitational field,

$$\frac{\partial \Omega}{\partial x} = - g \cos\theta \qquad \frac{\partial \Omega}{\partial y} = 0 \qquad \frac{\partial \Omega}{\partial z} = + g \sin\theta$$

Thus, the equations of motion reduce to

$$\rho \frac{\partial v_z}{\partial t} = -\rho g \sin\theta + \frac{\partial \sigma_{xz}}{\partial x}$$

Now, substituting the rheology equations into the previous,

$$\mu \frac{\partial^2 v_z}{\partial x^2} - \rho \frac{\partial v_z}{\partial t} = + \rho g \sin\theta \qquad \text{if} \quad |\sigma_{xz}| \geq \Phi$$

$$\frac{\partial v_z}{\partial x} = 0 \qquad \text{if} \quad |\sigma_{xz}| \leq \Phi$$

where the stress σ_{xz} at any position x is

$$\sigma_{xz} = + \rho g x \sin\theta + \rho \int_0^x \frac{\partial v_z}{\partial t} \, dx$$

with boundary conditions imposed by our assumptions:

$$v_z(L, t) = c(t)$$

$$\frac{\partial v_z(0, t)}{\partial x} = 0$$

Two flow conditions may now be realized: (1) if $|\sigma_{xz}| \leq \Phi$ everywhere in the fluid, then no flow will occur and the material acts as a solid; and (2) if $|\sigma_{xz}| > \Phi$ in only part of the material, then

local flow will occur in this (plastic) region and the remainder will behave as a solid. Unless $\Phi = 0$, it is not possible to have $|\sigma_{xz}| > \Phi$ everywhere in the material because the stress at the free surface must be zero. Thus, some of the material must behave as a solid if $\Phi > 0$.

The transition from elastic to plastic behavior takes place at the yield point where $|\sigma_{xz}| = \Phi$, or, denoting the occurrence of this transition to be at x^*,

$$\Phi = \left| + \rho g x^* \sin\theta + \rho \int_0^{x^*} \frac{\partial v_z}{\partial t} dx \right|$$

Thus, for values of $x > x^*$ there is a finite velocity gradient.

Dimensionless Form for the Equations

Starting with the general equations:

$$\mu \frac{\partial^2 v_z}{\partial x^2} - \rho \frac{\partial v_z}{\partial t} = + \rho g \sin\theta$$

$$\frac{\partial v_z}{\partial x} = 0$$

and using the transformations:

$$V = \frac{v_z}{v_0} \qquad T = \frac{\mu t}{\rho L^2} \qquad X = \frac{x}{L}$$

Then, in terms of dimensionless variables, the equations become

$$\frac{\partial^2 V}{\partial X^2} - \frac{\partial V}{\partial T} = + \frac{\rho g L^2}{\mu v_0} \sin\theta \qquad \text{if } |\sigma_{xz}| \geqslant \Phi$$

$$\frac{\partial V}{\partial X} = 0 \qquad \text{if } |\sigma_{xz}| \leqslant \Phi$$

with boundary conditions:

$$V(1, T) = c(T)$$

$$\frac{\partial V(0, T)}{\partial X} = 0$$

Using the additional transformation,

$$\sigma' = \frac{\sigma_{xz}}{\Phi}$$

the dimensionless form of the stress becomes

$$\sigma' = + \frac{\rho g L X \sin\theta}{\Phi} + \frac{\mu v_0}{L\Phi} \int_0^X \frac{\partial V}{\partial T} dX$$

Thus, the equations reduce to

$$\frac{\partial^2 V}{\partial X^2} - \frac{\partial V}{\partial T} = + \beta \qquad \text{if } |\sigma'| \geqslant 1$$

$$\frac{\partial V}{\partial X} = 0 \qquad \text{if } |\sigma'| \leqslant 1$$

and

$$\sigma' = \gamma X + \eta \int_0^X \frac{\partial V}{\partial T}\, dX$$

The dimensionless parameters of the system are

$$\gamma = \frac{\rho g L \sin\theta}{\Phi}$$

$$\eta = \frac{\mu v_0}{L\Phi}$$

$$\beta = \frac{\gamma}{\eta}$$

η is a dimensionless parameter first presented by Oldroyd (1947b) and sometime later given the name, Bingham Number. This number indicates the relative proportion of the viscous stress to the yield stress.

Transformation of Variables

For the dimensionless equation of motion where

$$|\sigma'| \geq 1$$

let

$$U + W = V$$

where U is a function which satisfies

$$\frac{\partial^2 U}{\partial X^2} = + \beta$$

such that the boundary conditions become

$$U(1) = 0$$

$$\frac{\partial U(X^*)}{\partial X} = 0$$

Then, W is a function which satisfies the condition

$$\frac{\partial^2 W}{\partial X^2} - \frac{\partial W}{\partial T} = 0$$

with boundary conditions:

$$W(1, T) = c(T)$$

$$\frac{\partial W(X^*, T)}{\partial X} = 0$$

Solution for U (Steady State Component of V)

U represents the component of flow which is a result of the force exerted on the fluid by the gravitational field only. It may be considered the steady state segment of the mucous flow or the condition of flow under ciliastasis (i. e., $c(t) = 0$). In the transformed notation,

$$\frac{\partial^2 U}{\partial X^2} = + \beta \qquad \text{if } |\sigma'| \geq 1$$

with boundary conditions:

$$U(1) = 0$$

$$\frac{\partial U(x^*)}{\partial X} = 0$$

The solution becomes

$$U = + \frac{\beta}{2} [X^2 - 1 + 2X^*(1 - X)]$$

Since

$$\frac{\partial U}{\partial X} = 0 \qquad \text{for } |\sigma'| \leqslant 1$$

then,

$$U(X) = U(X^*) \qquad \text{for } |\sigma'| \leqslant 1$$

Therefore, in total,

$$U = \mp \frac{\beta}{2} [X^2 - 1 + 2X^*(1 - X)] \qquad \text{if } |\sigma'| \geqslant 1$$

$$U = -\frac{\beta}{2} (1 - X^*)^2 \qquad \text{if } |\sigma'| \leqslant 1$$

Transforming back to a dimensional form:

$$U = -\frac{\rho g \sin\theta}{\mu} [L^2 - x^2 + 2x^*(x - L)] \qquad \text{if } |\sigma_{xz}| \geqslant \Phi$$

and

$$U = -\frac{\rho g \sin\theta}{\mu} [L^2 - x^{*2} - 2x^* L] \qquad \text{if } |\sigma_{xz}| \leqslant \Phi$$

However, if ciliastasis exists such that there is no periodic component to the velocity, i. e., $W = 0$, then

$$\sigma_{xz} = \mp x \rho g \sin\theta$$

Therefore,

$$x^* = \left|\frac{\Phi}{\rho g \sin\theta}\right|$$

Substituting x^* into U yields:

$$U = v_z = -\frac{\rho g \sin\theta}{2\mu}(L^2 - x^2) - \frac{\Phi}{\mu}(x - L)$$

and

$$U = v_z = -\frac{1}{\mu}\left[\frac{L^2 \rho g \sin\theta}{2} + \frac{\Phi^2}{2\rho g \sin\theta} - L\Phi\right]$$

However, the solution becomes the trivial case of $U = 0$ if

$$|\rho g L \sin\theta| \leq \Phi$$

Solution of W (Time-dependent Portion of V)

W is that portion of v_z which is a result of the movement of the cilia tips. The transformed equation is

$$\frac{\partial^2 W}{\partial X^2} - \frac{\partial W}{\partial T} = 0 \qquad \text{if } |\sigma'| \geq 1$$

with boundary conditions:

$$W(1, T) = c(T)$$

$$\frac{\partial W}{\partial X}(X^*, T) = 0$$

Essentially, the difficulty in the solution of this equation is in the determination of the unknown moving boundary X^*, the yield

surface. The non-linearity of the problem becomes more apparent with the transformation:

$$\zeta = \frac{1 - X}{1 - X^*}$$

Then the equation becomes

$$\frac{\partial^2 W}{\partial \zeta^2} - (1 - X^*)^2 \frac{\partial W}{\partial T} - \zeta(1 - X^*) \frac{\partial X^*}{\partial T} \frac{\partial W}{\partial \zeta} = 0$$

with boundary conditions:

$$W(0, T) = c(T)$$

$$\frac{\partial W}{\partial \zeta}(1, T) = 0$$

Now the non-linearity is shown by the fact that X^* and its derivative, which appear in the coefficients of the differential equation, depend on the solution by way of the equation:

$$\left| \gamma X^* + \eta \int_0^{X^*} \frac{\partial V}{\partial T} dX \right| = 1$$

Due to the non-linearity caused by the moving boundary a solution must be considered for each of the following cases:

I) when the movement of the yield surface is substantial; and

II) when the movement of the yield surface is negligible.

Case I

There are a number of physical problems, in addition to the one discussed in this thesis, which are governed by a parabolic differential equation in conjunction with a moving boundary condition (for example, when a material freezes, melts, or recrystallizes). Some of these problems have been investigated in recent years, and although specific ones have been undertaken with some success, no general theory for dealing with this type of problem has been developed.

The approach used in this investigation is generally similar to that used by Douglas and Gallie (1955) and by Ehrlich (1958). They dealt with parabolic differential equations with moving boundary conditions by utilizing an implicit difference technique in a numerical solution.

Using such a technique in this case, the solution lies in the space-time plane which is defined by the limits $0 \leqslant X \leqslant 1$ and $T \geqslant 0$. This $X - T$ plane may be considered as subdivided into a grid of equal rectangles with sides,

$h = \Delta X$, the mesh size in the space-direction, X

$\ell = \Delta T$, the mesh size in the time-direction, T

The finite difference equation of Crank and Nicolson:

$$\frac{W_{i,j+1} - W_{i,j}}{\ell} = \frac{1}{2}\left[\frac{W_{i+1,j+1} - 2W_{i,j+1} + W_{i-1,j+1}}{h^2} + \frac{W_{i+1,j} - 2W_{i,j} + W_{i-1,j}}{h^2}\right]$$

then rearranges to:

$$-rW_{i-1,j+1} + (2 + 2r)W_{i,j+1} - rW_{i+1,j+1} = rW_{i-1,j} + (2 - 2r)W_{i,j} + rW_{i+1,j}$$

where,

$X = ih$ $\qquad i = 0, 1, 2 \ldots$

$T = j\ell$ $\qquad j = 0, 1, 2 \ldots$

$r = \frac{\ell}{h^2}$

Using (N - 1) internal grid points along each time-row produces (N - 1) simultaneous Crank-Nicolson equations stated in terms of the boundary conditions and the known values at previous grid points.

In finite difference terms the boundary conditions become:

$$W_{n,j} = c(j)$$

$$W_{k+1,j} = W_{k-1,j}$$

where k is the mesh point closest to the yield surface, X^*.

The Crank-Nicolson equations for this problem are now written as follows:

a) at k,

$$(2 + 2r)W_{k, j+1} - 2rW_{k+1, j+1} = d_k$$

b) at $i = k + 1, \ldots N - 2$,

$$- rW_{i-1, j+1} + (2 + 2r)W_{i, j+1} - rW_{i+1, j+1} = d_i$$

c) at $N = 1$,

$$- rW_{N-2, j+1} + (2 + 2r)W_{N-1, j+1} = d_{N-1}$$

d) at N,

$$W_{N, j+1} = c(j + 1)$$

where the "d" values are:

a) for k,

$$d_k = (2 - 2r)W_{k, j} + 2rW_{k+1, j}$$

b) for $i = k + 1, \ldots N - 2$,

$$d_i = rW_{i-1, j} + (2 - 2r)W_{i, j} + rW_{i+1, j}$$

c) for $N - 1$,

$$d_{N-1} = (2 - 2r)W_{N-1, j} + r(W_{N-2, j} + W_{N, j} + W_{N, j+1})$$

The Gauss elimination method may be used to solve these Crank-Nicolson equations: the first equation is used to eliminate W_k from the second equation; the new second equation is used to eliminate W_{k+1} from the third equation; and so forth, until just one

equation exists with one unknown W_{N-1}. The unknowns W_{N-2}, W_{N-3}, . . . are then found by back substitution in a manner discussed by Smith (1965, p. 21). The resulting values of W_i are:

$$W_{k, j+1} = \frac{M_k + 2rW_{k+1, j+1}}{a_k}$$

and for $i = k + 1, \ldots N - 2$,

$$W_{i, j+1} = \frac{M_i + rW_{i+1, j+1}}{a_i}$$

and for $N - 1$,

$$W_{N-1, j+1} = \frac{M_{N-1}}{a_{N-1}}$$

where

$$M_k = d_k$$

and for $i = k + 1, \ldots N - 2$,

$$M_i = d_i + \frac{rM_i}{a_{i-1}}$$

$$a_k = 2 + 2r$$

$$a_{k+1} = (2 + 2r) - \frac{2r^2}{2 + 2r}$$

and for $i = k + 2, N - 1$

$$a_i = (2 + 2r) - \frac{r^2}{a_{i-1}}$$

It now becomes necessary to evaluate the position of the yield surface, X^*, which, as discussed previously, occurs when

$$\left| \gamma X^* + \eta \int_0^{X^*} \frac{\partial V}{\partial T} dX \right| = 1$$

or, in finite difference notation, when

$$\left| \gamma kh + \eta h \sum_{i=0}^{k} \left(\frac{W_{i,j+1} - W_{i,j}}{\ell} \right) \right| \simeq 1$$

This equation is approximately one, rather than equal to one, since it is unlikely that the yield surface will be exactly at a mesh point. Of course, as the mesh size approaches zero, this equation approaches unity.

The value of k may be determined through an iterative procedure as follows: First, an estimated value of k is used to evaluate solutions of W_i from the Crank-Nicolson equations. Then these solutions are used in the finite difference equation of the yield surface position. If the result does not achieve the required yield condition (i.e., in this case, unity), then k is increased by one and the procedure is repeated. On the other hand, if the result exceeds the required yield condition, the value of k is decreased by one and the procedure repeated. In this manner then, k converges toward the grid point nearest the actual yield surface. Rather than converging to and remaining at a grid point, however, k may oscillate between

adjacent points since the finite difference equation is not identically one. For finite values of ΔX, k may be approximated as that point at which the solution of the finite difference equation is closest to one.

Now the iterative procedure is reinitiated, increasing by one the time index, j, and using the value at the previous time step for the new estimate of k. By repeating this iterative procedure at each time index, the yield surface, k, and the corresponding velocities, W_i, may be evaluated.

Case II

When the movement of the yield surface is negligible, i.e., $\frac{\partial X}{\partial T} = 0$, the problem becomes simply a partial differential equation with time-dependent boundary conditions. This occurs if

$$\eta \int_0^{X^*} \frac{\partial V}{\partial T} dX << 1$$

which may be written in the form

$$\eta \left[\frac{\partial}{\partial T} \int_0^{X^*} V dX - \frac{\partial X^*}{\partial T} V(X^*) \right] << 1$$

However, in the interval $0 \leqslant X \leqslant X^*$, V is not a function of X. Therefore,

$$\frac{\partial}{\partial T} \int_0^{X^*} V dX = X^* \frac{\partial V(X^*)}{\partial T} + V(X^*) \frac{\partial X^*}{\partial T}$$

and thus,

$$\eta \int_0^{X^*} \frac{\partial V}{\partial T} dX = \eta X^* \frac{\partial V(X^*)}{\partial T}$$

Therefore, the condition necessary for a stationary yield surface becomes

$$\frac{\partial V(X^*)}{\partial T} << \frac{1}{\eta X^*}$$

However, generally

$$\frac{\partial c(T)}{\partial T} > \frac{\partial V(X^*)}{\partial T}$$

Thus, the movement of the yield surface becomes negligible when

$$\frac{\partial c(T)}{\partial T} << \frac{1}{\eta X^*}$$

When this condition exists, the solution for the time-dependent component of the velocity, W, may be achieved as follows:

Assuming that initially,

$$W(X, T) = 0$$

The Laplace transform of the differential equation for W is

$$\frac{\partial^2 W(X, S)}{\partial X^2} - SW(X, S) = 0$$

with boundary conditions:

$$\frac{\partial W(X, S)}{\partial X} = 0$$

$$W(1, S) = c(S)$$

The solution of the transformed equation is

$$W(X, S) = c_1 \sinh \sqrt{S}X + c_2 \cosh \sqrt{S}X$$

where

$$c_1 = c(S) \frac{\sinh \sqrt{S}X^*}{\cosh \sqrt{S}(1 - X^*)}$$

and

$$c_2 = c(S) \frac{\cosh \sqrt{S}X^*}{\cosh \sqrt{S}(1 - X^*)}$$

Therefore,

$$W(X, S) = c(S) \frac{\cosh(X - X^*) \sqrt{S}}{\cosh(1 - X^*) \sqrt{S}}$$

The oscillation of the tips of the cilia (represented in the model as a continuous wall) occurs in a periodic fashion that can be described by a Fourier series:

$$c(t) = a_0 + \sum_{n=1}^{\infty} a_n \cos \frac{2n\pi}{P} t + b_n \sin \frac{2n\pi}{P} t$$

The nondimensional form of this is

$$c(T) = A_0 + \sum_{n=1}^{\infty} A_n \cos \frac{2n\pi}{a} T + B_n \sin \frac{2n\pi}{a} T$$

where

$$A_0 = \frac{a_0}{v_0} \qquad A_n = \frac{a_n}{v_0} \qquad B_n = \frac{b_n}{v_0}$$

and

$$a = \frac{\mu P}{\rho L^2}$$

The parameter a is a dimensionless number sometimes referred to as Stokes Criterion and is essentially a modified Reynolds number for oscillatory flow.

The Laplace transform of the oscillation of the wall, $c(T)$, is

$$c(S) = \frac{A_0}{S} + \sum_{n=1}^{\infty} A_n \left[\frac{S}{S^2 + (\frac{2n\pi}{a})^2} \right] + B_n \left[\frac{(\frac{2n\pi}{a})}{S^2 + (\frac{2n\pi}{a})^2} \right]$$

Dealing first with the A_0 component of $c(S)$:

$$W_I(X, S) = \frac{A_0 \cos h \sqrt{S}(X - X^*)}{S \cos h \sqrt{S}(1 - X^*)}$$

The required inverse, $W_I(X, T)$, may be derived from Bromwich's integral formula and may be evaluated by the sum of residues at the poles when

$$|W(X, Re^{j\phi})| \to 0 \qquad \text{as } R \to \infty$$

(Savant, 1962)

Therefore, considering

$$S = Re^{j\phi}$$

then,

$$W_I(X, Re^{j\phi}) = \frac{A_0 \left[1 + e^{-2\sqrt{Re^{j\phi}}\,(X - X^*)}\right]}{Re^{j\phi}(1 - X^*)\left[1 + e^{-2\sqrt{Re^{j\phi}}(1 - X^*)}\right]}$$

Since, by definition,

$$X \leqslant 1$$

Then it is the case that

$$\left|W_I(X, Re^{j\phi})\right| \to 0 \quad \text{as} \quad R \to \infty$$

Therefore,

$$W_I(X, T) = \sum \text{ residues at the poles of } W_I(X, S)$$

The poles or singularities of $W_I(X, S)$ are at $S = 0$ and at

$$S = -\frac{\pi^2 (m + \frac{1}{2})^2}{(1 - X^*)^2} \qquad \text{for} \quad m = 0, 1, 2, \ldots .$$

At the pole $S = 0$, the residue is simply A_0. At the poles

$$S = -\frac{\pi^2 (m + \frac{1}{2})^2}{(1 - X^*)^2} \qquad \text{for} \quad m = 0, 1, 2, \ldots .$$

the residues are

$$\frac{2A_0}{\pi} \sum_{m=0}^{\infty} \frac{(-1)^m e^{-\frac{\pi^2(m+\frac{1}{2})}{(1-X^*)}T} \cos\left[\frac{(m+\frac{1}{2})\pi}{(1-X^*)}(X-X^*)\right]}{(1-X^*)(m+\frac{1}{2})}$$

This series is the transient term in the solution of $W_I(X, T)$, and since this thesis concerns only the steady periodic solution, this series will not be considered further. Therefore,

$$W_I(X, T) = A_0$$

Dealing now with the even components of c(S), that is, with the cosine terms:

$$W_{II}(X, S) = \sum_{n=1}^{\infty} A_n \left[\frac{S}{S^2 + (\frac{2n\pi}{a})^2}\right] \frac{\cosh \sqrt{S}(X - X^*)}{\cosh \sqrt{S}(1 - X^*)}$$

Here,

$$W_{II}(X, Re^{j\phi}) = \sum_{n=1}^{\infty} \frac{A_n}{[Re^{j\phi} + (\frac{2n\pi}{a})^2 e^{-j\phi}] e^{\sqrt{Re^{j\phi}}(1-X^*)}}$$

$$\cdot \left[\frac{1 + e^{-2\sqrt{Re^{j\phi}}(X - X^*)}}{1 + e^{-2\sqrt{Re^{j\phi}}(1 - X^*)}}\right]$$

Thus,

$$|W_{II}(X, Re^{j\phi})| \to 0 \qquad \text{as } R \to \infty$$

and so

$$W_{II}(X, T) = \sum \text{residues at the poles of } W_{II}(X, S)$$

The poles of $W_{II}(X, S)$ are at

$$S = \pm \frac{2n\pi i}{a} \qquad \text{for } n = 1, 2, \ldots .$$

and at

$$S = -\frac{\pi^2(m + \frac{1}{2})^2}{(1 - X^*)^2} \qquad \text{for } m = 0, 1, 2, \ldots .$$

For the poles at

$$S = -\frac{\pi^2(m + \frac{1}{2})^2}{(1 - X^*)^2} \qquad \text{for } m = 0, 1, 2, \ldots .$$

the residues are

$$\sum_{n=1}^{\infty} 2A_n \sum_{m=0}^{\infty} \frac{(-1)^m \pi^3 (m + \frac{1}{2})^3 e^{-\frac{\pi^2(m+\frac{1}{2})^2 T}{(1 - X^*)^2}} \cos\left[\frac{\pi(m + \frac{1}{2})}{(1 - X^*)} (X - X^*)\right]}{(1 - X^*)^4 \left[\left[\frac{\pi^2(m + \frac{1}{2})^2}{(1 - X^*)^2}\right]^2 + \left[\frac{2n\pi}{a}\right]^2\right]}$$

Again, this series may be neglected since only the steady periodic solution is being considered. For the poles at

$$S = \pm \frac{2n\pi}{a} i \qquad \text{for } n = 1, 2, \ldots .$$

the residues are

$$\sum_{n=1}^{\infty} \frac{A_n}{2} \left[e^{\frac{2n\pi}{a} iT} \frac{\cosh(1+i)\sqrt{\frac{n\pi}{a}}(X - X^*)}{\cosh(1+i)\sqrt{\frac{n\pi}{a}}(1 - X^*)} \right.$$

$$\left. + e^{-\frac{2n\pi}{a} iT} \frac{\cosh(1-i)\sqrt{\frac{n\pi}{a}}(X - X^*)}{\cosh(1-i)\sqrt{\frac{n\pi}{a}}(1 - X^*)} \right]$$

by identity,

$$\cosh(1 \pm i)\sqrt{\frac{n\pi}{a}}(X - X^*) = \cosh\sqrt{\frac{n\pi}{a}}(x - X^*)\cos\sqrt{\frac{n\pi}{a}}(X - X^*)$$

$$\pm i \sinh\sqrt{\frac{n\pi}{a}}(X - X^*)\sin\sqrt{\frac{n\pi}{a}}(X - X^*)$$

and thus,

$$\frac{\cosh(1 + i)\sqrt{\frac{n\pi}{a}}(X - X^*)}{\cosh(1 + i)\sqrt{\frac{n\pi}{a}}(1 - X^*)} = \Gamma(n, X)e^{i\Theta(n, X)}$$

where

$$\Gamma(n, X) = \left[\frac{\cosh 2\sqrt{\frac{n\pi}{a}}(X - X^*) + \cos 2\sqrt{\frac{n\pi}{a}}(X - X^*)}{\cosh 2\sqrt{\frac{n\pi}{a}}(1 - X^*) + \cos 2\sqrt{\frac{n\pi}{a}}(1 - X^*)}\right]\frac{1}{2}$$

and

$$\Theta(n, X) = \tan^{-1}\left[\tanh\sqrt{\frac{n\pi}{a}}(X - X^*)\tan\sqrt{\frac{n\pi}{a}}(X - X^*)\right]$$

$$- \tan^{-1}\left[\tanh\sqrt{\frac{n\pi}{a}}(1 - X^*)\tan\sqrt{\frac{n\pi}{a}}(1 - X^*)\right]$$

Also, by a similar argument:

$$\frac{\cosh(1 - i)\sqrt{\frac{n\pi}{a}}(X - X^*)}{\cosh(1 - i)\sqrt{\frac{n\pi}{a}}(1 - X^*)} = \Gamma(n, X)e^{-i\Theta(n, X)}$$

Therefore, the steady periodic solution of $W(X, T)$, derived from the even terms in $c(T)$, may be written:

$$\sum_{n=1}^{\infty} A_n \Gamma(n, X)\left[\frac{e^{i\left(\frac{2n\pi}{a} T + \Theta(n, X)\right)} + e^{-i\left(\frac{2n\pi}{a} T + \Theta(n, X)\right)}}{2}\right]$$

or,

$$\sum_{n=1}^{\infty} A_n \Gamma(n, X) \cos\left[\frac{2n\pi}{a} T + \Theta(n, X)\right]$$

The odd components of $c(S)$ must now be considered:

$$W_{III}(X, S) = \sum_{n=1}^{\infty} B_n \left[\frac{\frac{2n\pi}{a}}{S^2 + \left(\frac{2n\pi}{a}\right)^2}\right] \frac{\cosh \sqrt{S}\,(X - X^*)}{\cosh \sqrt{S}\,(1 - X^*)}$$

with poles at

$$S = \pm \frac{2n\pi}{a} i \qquad \text{for } n = 1, 2, \ldots .$$

and

$$S = -\frac{\pi^2 (m + \frac{1}{2})^2}{(1 - X^*)^2} \qquad \text{for } m = 0, 1, 2, \ldots .$$

Here again,

$$|W_{II}(X, Re^{j\phi})| \to 0 \qquad \text{as } R \to \infty$$

Evaluating residues at the poles

$$S = -\frac{\pi^2 (m + \frac{1}{2})^2}{(1 - X^*)^2} \qquad \text{for } m = 0, 1, 2, \ldots .$$

yields

$$\sum_{n=1}^{\infty} B_n \sum_{m=0}^{\infty} (-1)^m \frac{\pi(m+\frac{1}{2})[\frac{2n\pi}{a}]\, e^{-\frac{\pi^2(m+\frac{1}{2})^2 T}{(1-X^*)^2}} \cos[\frac{\pi(m+\frac{1}{2})}{(1-X^*)}(X-X^*)]}{(1-X^*)^2[[\frac{\pi^2(m+\frac{1}{2})^2}{(1-X^*)^2}]^2 + [\frac{2n\pi}{a}]^2]}$$

which, as before, is the transient term of the solution and need not be considered further.

For the poles at

$$S = \pm \frac{2n\pi}{a} i \qquad \text{for } n = 1, 2, \ldots .$$

evaluating the residues gives

$$\sum_{n=1}^{\infty} \frac{B_n}{2} \left[\frac{e^{\frac{2n\pi}{a} iT} \cosh(1+i)\sqrt{\frac{n\pi}{a}}(X-X^*)}{i \cosh(1+i)\sqrt{\frac{n\pi}{a}}(1-X^*)} \right.$$

$$\left. - \frac{e^{-\frac{2n\pi}{a} iT} \cosh(1-i)\sqrt{\frac{n\pi}{a}}(X-X^*)}{i \cosh(1-i)\sqrt{\frac{n\pi}{a}}(1-X^*)} \right]$$

Treating this as done previously yields:

$$\sum_{n=1}^{\infty} B_n \Gamma(n, X) \sin[\frac{2n\pi}{a} T + \Theta(n, X)]$$

Therefore, the complete steady periodic solution for $X \geq X^*$ is

$$W(X, T) = A_0 + \sum_{n=1}^{\infty} \Gamma(n, X) \left[A_n \cos\left(\frac{2n\pi}{a} T + \Theta(n, X)\right) \right.$$

$$\left. + B_n \sin\left(\frac{2n\pi}{a} T + \Theta(n, X)\right)\right]$$

And since

$$\frac{\partial W(X, T)}{\partial T} = 0 \qquad \text{for } X \leqslant X^*$$

then

$$W(X, T) = W(X^*, T) \text{ for } X \leqslant X^*$$

Therefore, for $X \geqslant X^*$

$$W(X, T) = A_0 + \sum_{n=1}^{\infty} \Gamma(n, X)\left[A_n \cos\left(\frac{2n\pi}{a} T + \Theta(n, X^*)\right)\right.$$

$$\left. + B_n \sin\left(\frac{2n\pi}{a} T + \Theta(n, X^*)\right)\right]$$

and for $X \leqslant X^*$

$$W(X, T) = A_0 + \sum_{n=1}^{\infty} \Gamma(n, X^*)\left[A_n \cos\left(\frac{2n\pi}{a} T + \Theta(n, X^*)\right)\right.$$

$$\left. + B_n \sin\left(\frac{2n\pi}{a} T + \Theta(n, X^*)\right)\right]$$

Thus, the time-dependent portion of the velocity, W, may be derived for either Case I or Case II. Finally then, the total velocity, V, is simply the sum of the steady state component, U, and the appropriate time-dependent component, W.

Programmed Model

In order to evaluate the effects on the system of parameter changes, the numerical solution for $\frac{dX^*}{dT} \gtrless 0$ and the analytical solution for $\frac{dX^*}{dT} \simeq 0$ were programmed in Fortran IV (Appendix) and run on a CDC 3300 computer at Oregon State University. By using a computer it was possible to observe the effects of c(t) and the dimensionless parameters α and η on the movement of the mucus and, thus, to evaluate the interrelationships between density (ρ), viscosity (μ), layer thickness (L), and critical shear (Φ) with regard to a particular cilia oscillation c(t).

For these computer runs the surface representing the cilia tips was considered to be in continuous contact with the viscid mucous layer in a configuration of the system as Lucas and Douglas (1934) represented it. The cilia were considered to be 7.5 microns long, oscillating through an arc of 60° at a frequency of 1500 beats per minute. The maximum velocity achieved by the tips of the cilia, then, was .123 cm/sec; this occurred midway through the effective stroke.

The oscillation of the cilia tips, c(t), was depicted as sinusoidal:

During the effective stroke,

$$c(t) = .123 \sin(\frac{4\pi}{P}t)$$

and during the recovery stroke,

$$c(t) = .0441 \sin(\frac{4\pi}{3P}t)$$

thus, resulting in a forward to reverse phase ratio of 1:3. The velocity and position profiles for the continuous surface were represented as in Figures 11 and 12.

By definition, the dimensionless period of oscillation is

$$\alpha = \frac{\mu P}{\rho L^2}$$

Now, since measurements of mucous viscosity (μ) range from 0.1 poises (Boyd and Lapp, 1946) to 250 poises (Denton, 1963); since the stroke frequency is 1500 beats per minute or the period (P) is .04 seconds; since mucous density (ρ) is approximately that of water (Boyd and Lapp, 1946); and since the thickness of the viscid mucous layer is equal to or greater than five microns; then values for α were taken in the range 1.6 to 1.6×10^5.

Also by definition, the dimensionless parameter

$$\eta = \frac{\mu v_o}{L\Phi}$$

In order to observe the system from the situation in which the yield surface, X^*, remains at zero to the situation in which X^* remains

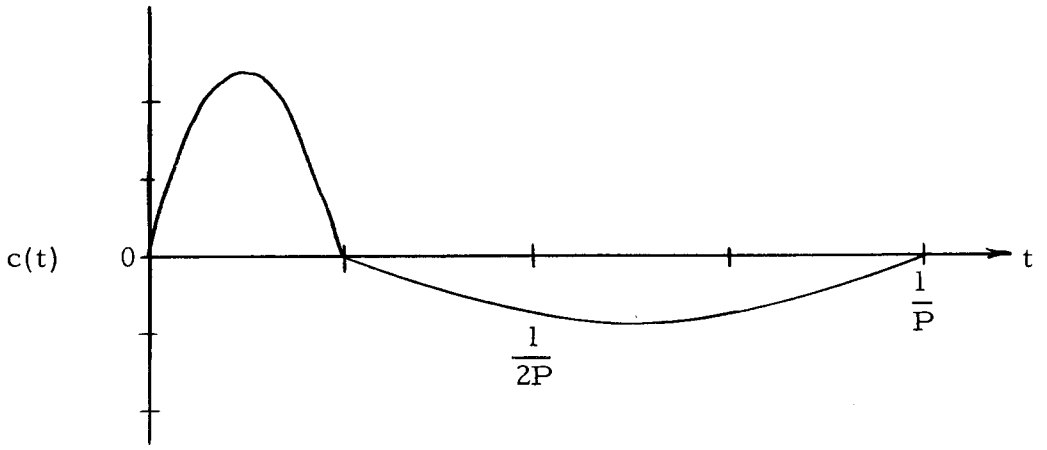

Figure 11. The velocity profile at the cilia tips.

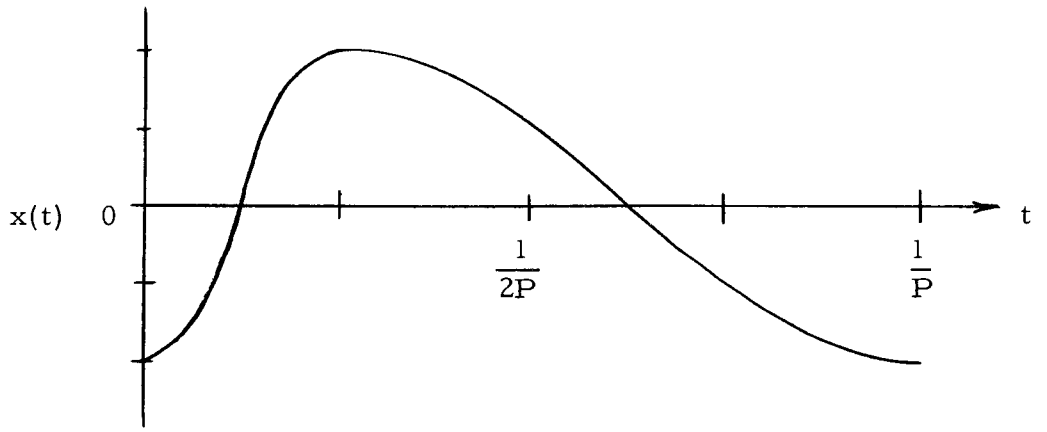

Figure 12. The position profile at the cilia tips.

at L, values of η were taken from .2 to 2×10^6. With a v_o of 1 cm/sec, this would correspond to a range of six orders of magnitude for Φ.

The numerical solution of the Crank-Nicolson equations has a truncation error of

$$-\frac{1}{12}(\Delta X)^2 \frac{\partial^4 V}{\partial X^4} + \frac{1}{6}(\Delta T)^2 \left[\frac{\partial^3 V}{\partial T^3} - \frac{3}{2}\frac{\partial^4 V}{\partial X^2 \partial T^2}\right] + \ldots .$$

Moreover, error may be introduced because of round-off within the computer. However, Smith (1965) indicated that for all values of r, that is $\frac{\Delta T}{(\Delta X)^2}$, the cumulative effect of all the rounding errors tends to zero as ΔX and ΔT tend to zero.

An additional error will be introduced in the moving boundary problem by estimating the position of X^* by a grid point which is in increments of ΔX. Thus, ΔX and ΔT should be taken as small as possible in order to minimize these errors.

For the situations considered, 100 increments were used in the X-coordinate and 4000 in the time-coordinate; therefore, $\Delta X = 0.01$ and $\Delta T = \frac{a}{4000}$.

No attempt was made to ascertain the exact magnitude of the errors; however, the numerical solution was checked with the analytical solution when possible and the answers were equal to four significant figures.

III. RESULTS AND CONCLUSIONS

In the model dimensionless parameters α, η, and γ were derived to represent combinations of the individual parameters ρ, μ, L, Φ, and P. Thus, the significant interrelationships of the individual parameters may be observed by evaluating the system under varying values of the dimensionless parameters.

From the basic equation $V = U + W$ several conditions of flow may be derived. When the angle of inclination θ is greater than zero such that the ciliated surface is inclined upwards, γ becomes greater than zero, the steady-state velocity U is negative, and thus any positive net velocity produced by the time-dependent portion W is diminished by the steady-state component. On the other hand, when θ is zero, γ is zero, and U is zero, and so the total velocity equals the time-dependent portion and the following flow conditions may exist:

The fluid behaves as a solid with a net velocity ($\overline{W}$) of zero if Φ is not exceeded at any time during an oscillation (Figure 13 and Table 1), i. e.,

$$\eta < \frac{1}{\frac{\partial V(X^*)}{\partial T}}$$

If Φ is exceeded during the effective stroke, i. e.,

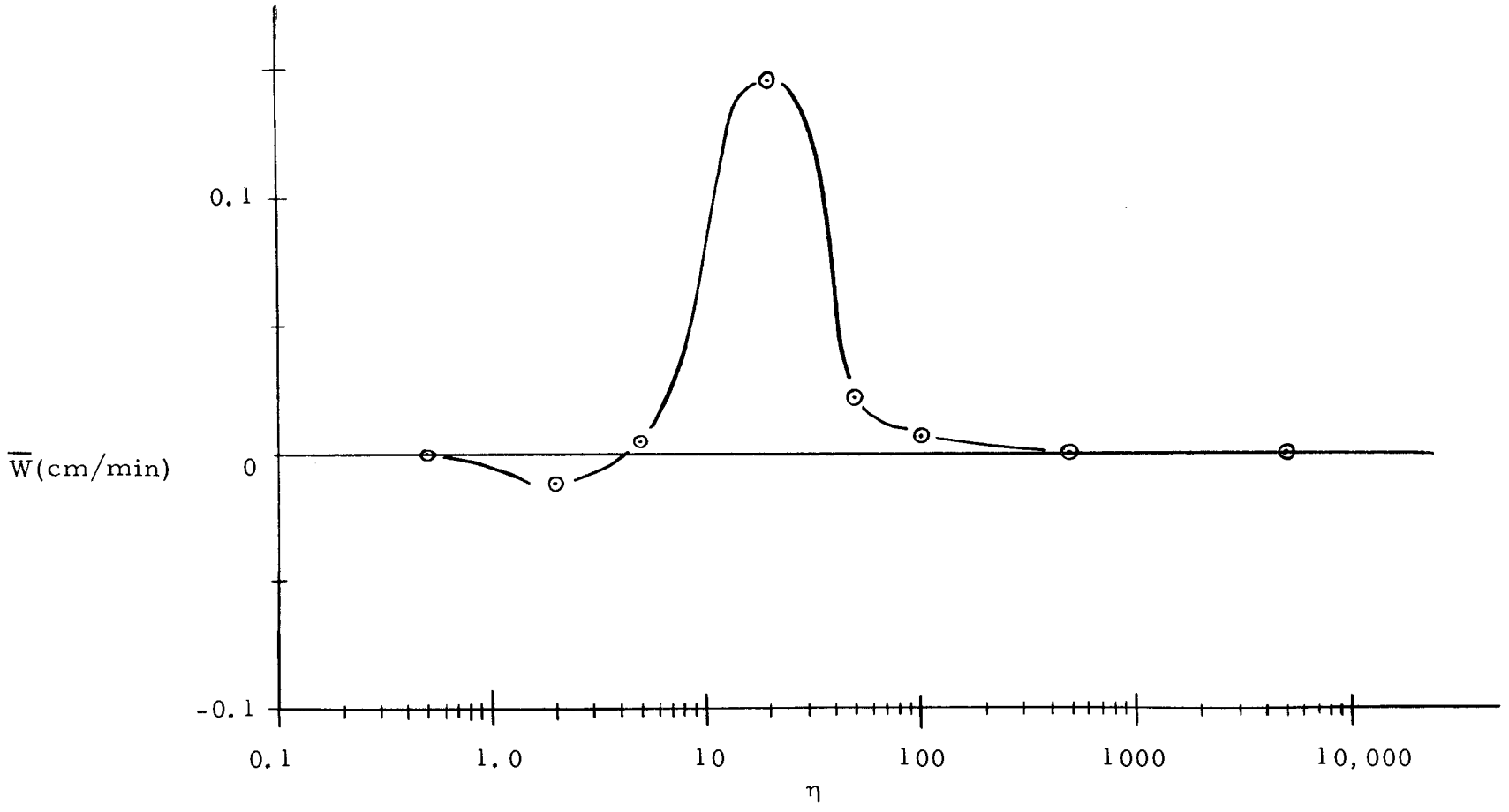

Figure 13. Net velocity of the viscid mucous layer for $\alpha = 1.6$ and $\theta = 0$.

Table 1. Average velocities (cm/min) for various positions of X under changing values for α and η with $\theta = 0$.

		X						
α	η	0	0.2	0.4	0.6	0.8	1.0	net V
	.05				zero			
	.5				zero			
	2	-.0133	-.0133	-.0133	-.0133	-.0133	zero	-.0127
	5	.0037	.0037	.0037	.0030	.0067	zero	.0042
1.6	20	.1759	.1759	.1835	.1702	.1060	zero	.1465
	50	.0080	.0141	.0342	.0300	.0160	zero	.0200
	200	-.0034	.0015	.0038	.0039	.0024	zero	.0021
	500				zero			
	5000				zero			
	1				zero			
	2.5				zero			
	25				zero			
	100	-.0026	-.0026	-.0025	-.0019	-.0010	zero	-.0010
40	250	-.0010	-.0009	-.0007	-.0003	zero	zero	-.0005
	1000	.0007	.0008	.0007	.0004	.0002	zero	.0005
	10,000	.0002	.0001	.0001	zero	zero	zero	.0001
	20				zero			
	50				zero			
	200	-.0001	-.0001	-.0001	zero	zero	zero	-.0001
	500				zero			
160	2000	.0001	.0001	.0001	.0001	zero	zero	.0001
	5000	.0001	.0001	.0001	zero	zero	zero	zero
	20,000				zero			
	5				zero			
	500				zero			
1,000	5000	slightly positive				zero	zero	zero
	50,000				zero			
	500,000				zero			
100,000	for all η				zero			

$$\eta > \frac{1}{\frac{\partial V_{eff}(X^*)}{\partial T}}$$

but is not exceeded during the recovery stroke, i. e. ,

$$\eta < \frac{1}{\frac{\partial V_{rec}(X^*)}{\partial T}}$$

then plastic flow occurs in the positive direction while the material moves as a solid in the negative direction. The resultant phase shift and reduction in velocity during the positive forward stroke may cause a small negative net velocity.

If Φ is exceeded in both the effective and recovery portions of the oscillation, and if during a portion of the forward stroke X^* is less than during the reverse stroke such that there is more plastic flow in the forward stroke, then because of the non-linear movement of X^*, the cumulative effect of the phase lag and diminution in velocity is greater during the reverse stroke, and thus the final result is a positive net velocity.

When Φ is exceeded during both phases and the position of the yield surface X^* is approximately the same during both phases (i. e. , $X^* \simeq 0$) then the movement of the material is similar to Newtonian flow and the net velocity is zero.

It is important to note that for very large values of α the

effective net velocity ($\overline{W}$) is zero regardless of the value of Φ or of the action and position of the yield surface X^*. In fact, using values which are considered to be normal for the individual parameters results in a value in the order of 10×10^4, and thus for the c(t) used for these solutions, no positive flow was achieved. If indeed this is a normal value for α, then it appears that in order to gain a positive flow, the cilia tips cannot be in continuous contact with the upper viscid layer (as assumed in the solutions presented), but instead must dip into the serous fluid during the recovery stroke.

If this conclusion is accurate, then, the serous layer of the mucous blanket is of much greater importance to the clearance mechanism than hitherto believed. When ciliastasis or mucostasis is caused by a decrease in the thickness of the mucous blanket (Bang, 1961), it may be the level of the serous fluid rather than the level of the viscid layer that is of greater significance; if the serous fluid becomes too thin the tips of the cilia would be in continuous contact with the viscid layer which, as the model indicates, would result in zero or even negative velocities. On the other hand, when mucous velocity decreases due to an increase in the thickness of the mucous blanket (Dalhamn, 1956), again it may be the level of the serous fluid that is more significant, since if the level is too great the tips of the cilia may not extend into the viscid layer at all.

Furthermore, for such a large value of α, the phase lag and

diminution of velocity across the fluid is already negligible, so that an increase in α due to an increase in μ has little or no additional effect. The viscosity of the upper viscid layer, therefore, may not be as important as previously believed.

As a result of these conclusions then, a few suggestions may be formulated regarding future research in this area:

First, the serous layer, which has been almost completely neglected in previous investigations, should be studied thoroughly in order to discover its actual physical properties and to observe the manner by which it relates to mucous flow and ciliary action under normal and pathological conditions.

Secondly, although the upper viscid layer has been the subject of numerous investigations, much has yet to be learned about it. Specifically, the rheology of this layer should be studied more carefully in order to determine whether treating the mucus as a Bingham plastic sufficiently describes its flow characteristics.

Finally, in reference to models of the system, a two-dimensional model should be developed in order to evaluate the effects, if any, of the metachronal wave.

BIBLIOGRAPHY

American Public Health Association. 1959. Resolutions: Lung cancer and cigarette smoking. American Journal of Public Health 49:1698.

Ballenger, John Jacob. 1949. A study of ciliary activity in the respiratory tract of animals. Annals of Otology, Rhinology and Laryngolgy 58:351-369.

Ballenger, John Jacob. 1960. Experimental effect of cigarette smoke on human respiratory cilia. The New England Journal of Medicine 263:832-835.

Ballenger, John Jacob and Mary Faith Orr. 1963. Quantitative measurement of human ciliary activity. Annals of Otology, Rhinology and Laryngology 72:31-39.

Bang, Frederick B. 1961. Mucociliary function as protective mechanism in upper respiratory tract. Bacteriological Reviews 25:228-236.

Barnett, B. and C. E. Miller. 1966. Flow induced by biological mucociliary systems. Annals of the New York Academy of Sciences 130:891-901.

Battigelli, Mario C. et al. 1966. Mucociliary activity. Archives of Environmental Health 12:460-466.

Bingham, Eugene C. 1916. An investigation of the laws of plastic flow. In: Scientific Papers of the National Bureau of Standards. Vol. 13, no. 278. Washington, D. C., Government Printing Office. p. 309-353.

Blake, James M. 1964. A facet of chronic respiratory disease. New York State Journal of Medicine 64:1727-1730.

Bloom, William and Donald W. Fawcett. 1964. A textbook of histology. Philadelphia, Saunders. 720 p.

Boyd, Eldon M. and M. Shirley Lapp. 1946. On the expectorant action of parasympathomimetic drugs. Journal of Pharmacology and Experimental Therapeutics 87:24-36.

Carson, S., R. Goldhamer and M. S. Weinberg. 1966. Characterization of physical, chemical and biological properties of mucus in the intact animal. Annals of the New York Academy of Sciences 130:935-943.

Dalhamn, Tore. 1956. Mucous flow and ciliary activity in the trachea of healthy rats and rats exposed to respiratory irritant gases. Acta Physiologica Scandinavica (sup. 123) 36:1-161.

Dalhamn, Tore and Johannes Rhodin. 1956. Mucous flow and ciliary activity in the trachea of rats exposed to pulmonary irritant gas. British Journal of Industrial Medicine 13:110-113.

Dalhamn, Tore and Ragnar Rylander. 1964. Ciliastatic action of smoke from filter-tipped and non-tipped cigarettes. Nature 201:401-402.

Dalhamn, Tore and Ragnar Rylander. 1966. Cigarette smoke and ciliastasis. Archives of Environmental Health 13:47-50.

Denton, Robert. 1963. The rheology of human lung mucus. Annals of the New York Academy of Sciences 106:746-754.

Douglas, Jim and T. M. Gallie. 1955. On the numerical integration of a parabolic differential equation subject to a moving boundary condition. Duke Mathematics Journal 22:557-571.

Ehrlich, L. W. 1958. A numerical method of solving a heat flow problem with moving boundary. Journal of the Association for Computing Machines 5:161-176.

Engström, H. and J. Wersäll. 1952. Some principles in the structure of vibratile cilia. Annals of Otology, Rhinology and Laryngology 61:1027-1038.

Gross, Paul. 1964. The processes involved in the biologic aspects of pulmonary deposition, clearance, and retention of insoluble aerosols. Health Physics 10:995-1002.

Hahn, Sang Joon, Taikyue Ree and Henry Eyring. 1959. Flow mechanism of thixotropic substances. Industrial and Engineering Chemistry 51:856-857.

Hatch, Theodore F. 1961. Distribution and deposition of inhaled particles in respiratory tract. Bacteriological Reviews 25:237-240.

Hatch, Theodore F. and Paul Gross. 1964. Pulmonary deposition and retention of inhaled aerosols. New York, Academic. 192 p.

Hilding, A. C. 1957. Ciliary streaming in the bronchial tree and the time element in carcinogenesis. The New England Journal of Medicine 256:634-640.

Hilding, A. C. 1963. Phagocytosis, mucous flow, and ciliary action. Archives of Environmental Health 6:61-73.

Hilding, A. C. 1965. Mucociliary insufficiency and its possible relation to chronic bronchitis and emphysema. Medicina Thoracalis 22:329-345.

Lamb, Horace. 1945. Hydrodynamics. 6th ed. New York, Dover. 738 p.

Landahl, H. D. 1950. On the removal of air-borne droplets by the human respiratory tract. Bulletin of Mathematical Biophysics 12:43-56.

Lucas, Alfred M. 1932. Ciliated epithelium. In: Special cytology, ed. by Edmund V. Cowdry. 2d ed. Vol. 1. New York, Hoeber. p. 408-473.

Lucas, Alfred M. and L. C. Douglas. 1934. Principles underlying ciliary activity in the respiratory tract. Archives of Otolaryngology 20:518-541.

McKennell, R. 1954. A versatile cone and plate viscometer with automatic flow curve recording. In: Proceedings of the Second International Congress of Rheology, Oxford, 1953. London, Butterworth. p. 350-359.

Merrill, Edward W. 1955. Basic problems in the viscometry of non-Newtonian fluids. Journal of the Instrument Society of America 2:462-465.

Merrill, Edward W. and Roe E. Wells, Jr. 1961. Flow properties of biological fluids. Applied Mechanics Reviews 14:663-673.

Miller, C. E. and H. Goldfarb. 1965. An in vitro investigation of ciliated activity. Transactions of the Society of Rheology 9:135-144.

Mitchell, Ralph I. and Joseph F. Tomashefski. 1964. Aerosols and the respiratory tract. Battelle Technical Review 13(1):3-8.

Morrow, Paul E. 1967. Adaptations of the respiratory tract to air pollutants. Archives of Environmental Health 14:127-136.

Oldroyd, J. G. 1947a. A rational formulation of the equations of plastic flow for a Bingham solid. Proceedings of the Cambridge Philosophical Society 43:100-105.

Oldroyd, J. G. 1947b. Two-dimensional plastic flow of a Bingham solid. Proceedings of the Cambridge Philosophical Society 43:383-395.

Oregon State Board of Health. 1958. Resident deaths from selected causes. In: Statistical supplement to the 28th Biennial Report, 1956-57. Salem, Oregon. Table 42.

Oregon State Board of Health. 1966. Resident deaths for selected causes. In: Oregon Public Health Statistical Report, 1965. Salem, Oregon. Table 25.

Proctor, Donald F. 1964. Physiology of the upper airway. In: Handbook of physiology, ed. by Wallace O. Fenn and Hermann Rahn. Vol. 1. Washington, D. C., American Physiological Society. p. 309-345.

Proetz, Arthur W. 1934. Nasal ciliated epithelium, with special reference to infection and treatment. The Journal of Laryngology and Otology 49:557-569.

Proetz, Arthur W. 1953. Essays on the applied physiology of the nose. 2d. ed. St. Louis, Annals. 452 p.

Rhodin, Johannes and Tore Dalhamn. 1956. Electron microscopy of the tracheal ciliated mucosa in rat. Zeitschrift für Zellforschung 44:345-412.

Rivera, Jose' A. 1962. Cilia, ciliated epithelium, and ciliary activity. New York, Pergamon. 167 p.

Savant, C. J., Jr. 1962. Fundamentals of the Laplace transformation. New York, McGraw-Hill. 229 p.

Smith, G. D. 1965. Numerical solution of partial differential equations. New York, Oxford University. 179 p.

Toremalm, N. G. 1960. The daily amount of tracheo-bronchial secretions in man: a method for continuous aspiration in laryngectomized and tracheotomized patients. Acta Otolaryngology (Sup.) 158:43-53.

U. S. Dept. of Health, Education, and Welfare. 1953. Deaths from 255 selected cases. In: Vital Statistics of the U. S., 1950. Vol. 3. Washington, D. C. Table 54.

U. S. Dept. of Health, Education, and Welfare. 1966. Deaths and death rates for each cause. In: Vital Statistics of the U. S., 1964. Vol. 2, part A. Washington, D. C. Table 1-22.

U. S. Weather Bureau. 1964. Storm data. Ashville, North Carolina, Jan.-Dec. 1964. (Totals compiled from monthy issues.)

Villee, Claude A. 1960. Biology. Philadelphia, Saunders. 615 p.

Wells, Roe E., Robert Denton and Edward W. Merrill. 1961. Measurement of viscosity of biologic fluids by cone plate viscometer. Journal of Laboratory and Clinical Medicine 57:646-656.

White, J. C. and P. C. Elmes. 1960. Some rheological properties of bronchial mucus and mucoprotein. In: Flow properties of blood and other biological systems, ed. by A. L. Copley and G. Stainsby. New York, Pergamon. p. 259-286.

APPENDICES

NUMERICAL SOLUTION FOR W(X,T)

THETA = 0

```
      PROGRAM CILIA  (NUMERICAL)
      REAL NU
      DIMENSION ALPH(101), D(101), S(101), U(101),
     1 AVE(101),W(101)
  300 FORMAT(2I6,4F12.4)
  310 FORMAT(1H0,3I6/(10F12.8))
  320 FORMAT(1H-,2X,11F12.8)
  330 FORMAT(1H-,5X,F12.8)
  340 FORMAT(1H1,2I6,5F12.4)
      READ(60,300)M,N,PERIOD,CRSHEAR,GAMA
      NU=GAMA/CRSHEAR
      WRITE(61,340)M,N,PERIOD,CRSHEAR,GAMA,NU
      DELT=PERIOD/M
      DELX=1.00/(N-1.00)
      R=DELT/(DELX*DELX)
      O=2-2*R
      P=2+2*R
      Q=R*R
      A=3*PERIOD/8
      B=5*PERIOD/8
      C=4.1887902/PERIOD
      F=12.5663706/PERIOD
      E=2.09439
      G=GAMA*DELX/(CRSHEAR*DELT)
      NONE=N-1
      NTWO=N-2
      DO 3 I=1,N
      AVE(I)=0
      D(I)=0
      S(I)=0
      U(I)=0
      W(I)=0
      IN=0
    3 ALPH(I)=0
      GAVE=0
      K=N
      J=1496
      UU=-0.00017203
      DO 5 I=1,N
    5 W(I)=UU
```

```
 10 IF(J .GT. M)800,801
800 T=(J-M)*DELT
    GO TO 802
801 T=J*DELT
802 CONTINUE
    IF(T .LT. A)13,11
 11 IF(T .LT. B)14,15
 13 WN=-0.04112*COSF(C*T)
    GO TO 16
 14 WN=0.12336*COSF(F*T)
    GO TO 16
 15 WN=-0.04112*COSF(C*T+E)
 16 KONE=K+1
    KTWO=K+2
    KSUB=K-1
    NK=N-K-1
    IF(K .EQ. N-1)200,210
210 IF(K .EQ. N)31,17
 17 ALPH(K)=P
    ALPH(K+1)=P-2*Q/P
    DO 18 I=KTWO,NONE,1
 18 ALPH(I)=P-Q/ALPH(I-1)
    D(K)=2*R*W(K+1)+O*W(K)
    DO 19 I=KONE,NTWO,1
 19 D(I)=R*W(I-1)+O*W(I)+R*W(I+1)
    D(N-1)=R*W(N-2)+O*W(N-1)+R*W(N)+R*WN
    S(K)=D(K)
    DO 20 I=KONE,NONE,1
 20 S(I)=D(I)+R*S(I-1)/ALPH(I-1)
    U(N-1)=S(N-1)/ALPH(N-1)
    DO 30 II=2,NK,1
    I=N-II
 30 U(I)=(S(I)+R*U(I+1))/ALPH(I)
    U(K)=(S(K)+2*R*U(K+1))/ALPH(K)
    GO TO 250
200 U(K)=(2*R*W(N)+O*W(K)+2*R*WN)/P
250 CONTINUE
 31 U(N)=WN
    DO 40 I=1,KSUB,1
 40 U(I)=U(K)
    BB=0.0
    DO 50 I=1,KSUB
 50 BB=BB+U(I)-W(I)
    CHECK=G*ABS(BB)
    IF(CHECK-1)73,80,74
 73 IF(IN .EQ. 2 .OR. K .EQ. N)80,75
```

```
 75 IN=1
    K=K+1
    GO TO 16
 74 IF(IN .EQ. 1 .OR. K .EQ. 1)80,76
 76 IN =2
    K=K-1
    GO TO 16
 80 DO 89 I=1,N
 89 W(I)=U(I)
    IF(J .GE. M)510,92
510 DO 90 I=1,N
 90 AVE(I)=AVE(I)+U(I)
    JJ=J/4
    IF(4*JJ .EQ. J)91,92
 91 WRITE(61,310) J,N,K,(U(I),I=1,N,10)
 92 J=J+1
    IN=0
    IF(J .LT. 2*M)10,100
100 DO 101 I=1,N
101 AVE(I)=AVE(I)*60/M
    WRITE(61,320) (AVE(I),I=1,N,10)
    DO 110 I=2,NONE,1
110 GAVE=GAVE+AVE(I)
    GAVE=GAVE+(AVE(1)+AVE(N))/2
    GAVE=GAVE/(N-1)
    WRITE(61,330) GAVE
    CALL EXIT
    END
       FINIS
```

ANALYTICAL SOLUTION FOR W(X,T)

THETA = 0

```
      PROGRAM CILIA  (ANALYTICAL)
      REAL NU
      DIMENSION ACON(40),BCON(40),RX(101),
     1 THETX(101),AVE(101)
  100 FORMAT(1H1)
  300 FORMAT(2I6,5F12.4)
  310 FORMAT(1H0,3I6/(10F12.8))
  340 FORMAT(1H1,2I6,5F12.4)
  400 FORMAT(2F12.8)
  500 FORMAT (1H-,11F12.4)
  600 FORMAT(1H-,F20.4)
   63 FORMAT(1H,2F12.6)
      READ(60,300)M,N,PERIOD,CRSHEAR,GAMA,XUMB
      NU=GAMA/CRSHEAR
      WRITE(61,340)M,N,PERIOD,CRSHEAR,GAMA,NU
      READ(60,400)XSTAR,VELCON
      NN=XSTAR*100
      DO 4 I=1,N
      VEL(I)=0
    4 AVE(I) = 0
      DELT=PERIOD/M
      SUM = 0.
      NUMB = XUMB
      DO 5 L=1,NUMB
      Z=L
      ZZ=Z**2
     1 (1/(4-ZZ)-1/(4-9*ZZ))
      ACON(L) = 1.90986*VELCON*(1+COSF(4.7124*Z))*
      BCON(L) = 0.95493*VELCON*(SINF(4.7124*Z))*
     1 (2/(4-ZZ)-2/(4-9*ZZ))
    5 WRITE(61,63) ACON(L),BCON(L)
      DO 78 J=1,M
      K=J-1
      T = DELT*K
      DO 75 I=NN,N
      X = (I-1.)/100.
      VSUM = 0
   25 DO 30 L=1,NUMB
      ARG = SQRTF(3.14159 *L/PERIOD)
      A=EXPF(ARG*(X-XSTAR))
      B=EXPF(ARG*(1-XSTAR))
```

```
      C=EXPF(-ARG*(X-XSTAR))
      D=EXPF(-ARG*(1-XSTAR))
      THETX(I)=ATAN((A-C)/(A+C)*SINF(ARG*(X-XSTAR))/
     1 COSF(ARG*(X-XSTAR)))-ATAN((B-D)/(B+D)*
     2 SINF(ARG*(1-XSTAR))/COSF(ARG*(1-XSTAR)))
      A=EXPF(2*ARG*(X-XSTAR))
      B=EXPF(2*ARG*(1-XSTAR))
      C=EXPF(-2*ARG*(X-XSTAR))
      D=EXPF(-2*ARG*(1-XSTAR))
      RX(I)=SQRTF(((A+C)/2+COSF(2*ARG*(X-XSTAR)))/((B+D)/2
     1 +COSF(2*ARG*(1-XSTAR))))
      ARG = 6.28318 * L/ PERIOD
      RESID=RX(I)*(ACON(L)*COSF(ARG*T+THETX(I))
     1 BCON(L)*SINF(ARG*T+THETX(I)))
   30 VSUM = VSUM +RESID
   75 VEL(I)=VSUM
      DO 76 I=1,NN
   76 VEL(I)=VEL(NN)
      DO 77 I=1,N
   77 AVE(I)=AVE(I)+VEL(I)
      JJ=J/4
      IF(4*JJ .EQ. J)50,78
   50 WRITE(61,310)J,N,NN,(VEL(I),I=1,N,10)
   78 CONTINUE
      DO 80 I=1,N
      AVE(I)=AVE(I)*60/M
   80 SUM = SUM+AVE(I)
      SUM=SUM/N
      PRINT 100
      PRINT 500, AVE
      PRINT 600,SUM
      CALL EXIT
      END
         FINIS
```